nature geoscience
SUPPLEMENTARY INFORMATION
DOI: 10.1038/NGEO1661

The impact of polar mesoscale storms on northeast Atlantic Ocean circulation

Atmospheric forcing fields

Our atmospheric forcing fields are based upon ERA-40 reanalyses data from the European Centre for Medium-range Weather Forecasts (ECMWF)[27]. These have a spatial resolution of 1.125°, but are linearly interpolated to a resolution of 0.25° for the NE Atlantic to generate a set of high-resolution Control and Perturbation forcing fields. Previous work[2] has shown that in the Control fields around 75% of polar lows <500 km in scale are missing. So, for the Perturbation fields, a polar low parameterization scheme[10] has been adapted to add these unresolved polar lows to the NE Atlantic in a realistic fashion. In brief: (i) at each model forcing-step the locations of all polar lows in the domain are determined using a cyclone detection algorithm[28]; (ii) a Rankine vortex is then inserted into the wind field at these locations, with the magnitude of the wind speed perturbation determined by the size of the vortex[10]; (iii) a bulk flux algorithm is used along with the model's sea-surface temperature and the perturbed wind field to recalculate the surface momentum and heat fluxes. An illustration of the polar low parameterization is shown in **Supplementary Figure 1.**

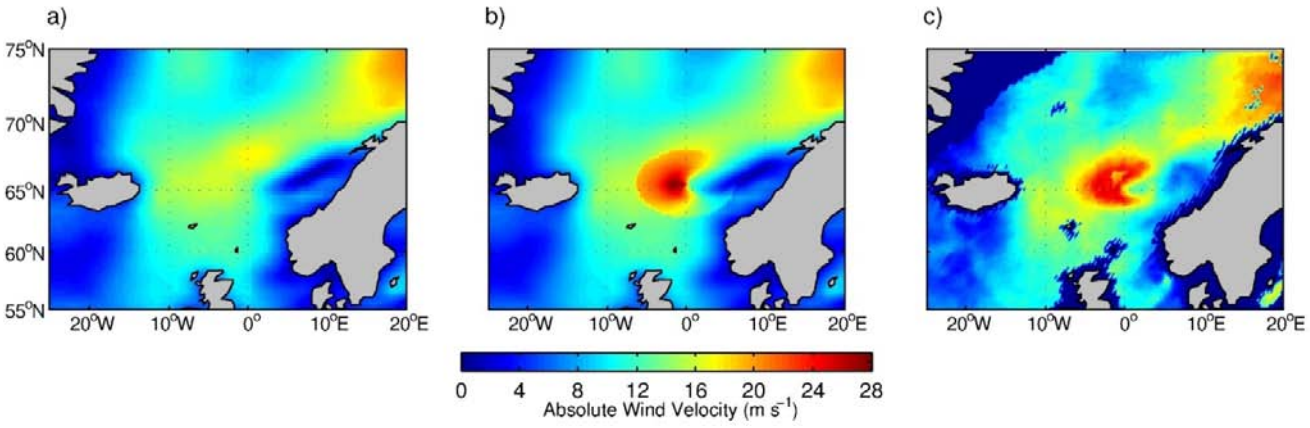

Supplementary Figure 1 | An illustration of the polar low parameterization. Panels show the surface wind speed at 06:00 UTC 15 October 1993 for: **a)** Standard ERA-40 data; **b)** ERA-40 with a polar low parameterized; and **c)** satellite data (morning pass) from Special Sensor Microwave/Imager (SSM/I) satellite data, NASA Pathfinder Mission (www.remss.com). The satellite data reveal a polar low over the Norwegian Sea with a diameter of ~400 km. The standard ERA-40 reanalysis do not capture the structure or magnitude of the wind field of this vortex. Parameterizing the vortex produces a considerably more accurate wind field.

To expand, the polar low parameterization scheme is based on that of Condron et al.[10], adapted to use a cyclone detection algorithm[28] to locate the polar mesoscale cyclones (here called polar lows) in

DOI: 10.1038/NGEO1661

ECMWF ERA40 reanalyses fields. The cyclone detection algorithm finds maxima in the Laplacian of mean-sea-level pressure (equivalent to geostrophic relative vorticity maxima) and distinguishes between 'open' and 'closed' cyclones. 'Closed' cyclones possess a region of closed isobars on a synoptic chart, and typically identify synoptic-scale (>500 km) cyclones; 'open' cyclones do not have a region of closed isobars and instead typically identify weaker mesoscale (<500 km) cyclones[2,28]. Here we use only open cyclones and a Laplacian threshold of 1.5 hPa/degree^2 to determine a polar low distribution that corresponds closely with independent climatologies[4-7] (see **Fig. 2**). Restricting the reanalysis data spatially and temporally to match a satellite climatology[5] we detect 3126 vortices (compared to 3179 in the satellite data set), with temporal and spatial correlation coefficients of *0.82* and *0.75* respectively. The strength of the parameterized vortices are determined using a linear relationship with vortex size[10], with the size distribution of the inserted vortices chosen to match observations[5]. This approach means the larger parameterized polar lows (300-500 km) have a much greater impact than the smaller ones (<300 km).

Parameterization Verification

The skill of the cyclone detection algorithm in accurately identifying polar lows in reanalysis data has been demonstrated previously[2]. As implemented here, there is a good temporal ($r = 0.82, p < 0.01$) and spatial ($r = 0.75, p < 0.01$) agreement between polar lows detected in ERA-40 and those recorded in a 2-year satellite-based climatology[5]. The ability of the parameterization to accurately reproduce the wind field of a typical polar low is illustrated in **Supplementary Fig. 1**. Satellite derived wind speed from 15 October 1993 illustrate a polar low over the Norwegian Sea with a diameter of ~400 km. This vortex has an average (maximum) wind speed of 15.6 m s^{-1} (25.4 m s^{-1}). Despite this vortex being identified as a weak disturbance by the cyclone detection algorithm, the standard ERA-40 reanalysis wind field does not resolve this feature, and as a result the average and maximum wind speed in the vicinity of the vortex (12.7 m s^{-1} and 14.7 m s^{-1}, respectively) are not distinguishable from the background wind field. Parameterizing the polar low produces a dramatic improvement in the quality of the wind field. The average (maximum) wind speed over the area of the vortex is now 14.7 m s^{-1} (27.8 m s^{-1}), close to the observations, and the maximum velocity is located to the west of the centre, as observed. This realistic wind field increases the total (latent plus sensible) heat loss from the ocean to the atmosphere by >500 W m^{-2} (to 988 W m^{-2}) over the area of maximum wind speed.

This case represents one example of many thousands of polar mesoscale cyclones parameterized in our Perturbation forcing fields. On average the polar low parameterization increases heat loss from the ocean to the atmosphere in the vicinity of individual storms by >200 W m^{-2}, reproducing localized heat fluxes that are in line with aircraft observations[9]. It is worth emphasizing that the annual mean area-

average difference in surface heat fluxes over the NE Atlantic for all the winters (DJFM) is modest in comparison (only 3 W m^{-2}; 3 %). However the intense nature of the forcing from individual storms has a significant impact on the ocean.

Further verification for the inclusion of polar lows is provided by a spectral analysis of the near-surface wind field for a month of data (**Figure 2).** The spectra are averages over approximately 20,000 lines. The Control (without polar lows) spectrum has a slope consistent with power cascading from larger to smaller scales, but far too little power at scales below ~300 km due to an inability of the atmospheric forcing fields to resolve storms below this scale. This lack of power at smaller scales is a well-known deficiency of numerical weather prediction modelling systems[e.g.29]. Indeed, it has been argued that the point of drop-off in these spectra can be used as a measure of the model's "effective resolution"[30] – in this case around 300-400 km. The Perturbation (with polar lows) spectrum has considerably more power between 50-400 km, bringing it remarkably into line with what is observed[18-19]; and implying the Perturbation experiment will be receiving the correct amount of wind forcing at scales of 50-400 km. Note there appears to be too much power in both model spectra at scales of 500-1000 km, compared to the observed power-law fits. However this distribution is consistent with this Nordic Seas domain being at the tail of the North Atlantic storm track and so having elevated wind speed variance at these scales[31]. This feature is reproduced in independent spectral analysis of other numerical weather prediction models (not shown).

A comparison to the pilot study

The question of whether polar lows can influence the circulation of the ocean was first examined by Condron et al.[10] who used a coarse spatial resolution (1-2°) and relatively simple numerical ocean model to run 2-year Perturbation and Control experiments, with the Perturbation run including polar lows over the Northeast Atlantic. Their methodology made use of a satellite-based polar low climatology to determine the location of the polar lows. This approach limited the experiments to two years and meant a thorough examination of the ocean impacts of polar lows was not possible; their "pilot study" was the first to highlight the potential importance between short-lived, intense mesoscale atmospheric activity (polar lows) and deep ocean circulation. Their results showed some monthly increases in GSDW production in response to more active open-ocean convection in the Nordic Seas, a spin up of the Nordic Seas gyre and a small (~2%) increase in the volume transport of deep water overflowing the Denmark Strait. However none of their results were statistically significant due to the limited extent of the simulations and the high variability of their GSDW formation rate. Our results are qualitatively consistent with the findings of their pilot study. However, the relatively high resolution we employ allows for a much better representation of the boundary currents and deep-water overflows of the Nordic Seas and

DOI: 10.1038/NGEO1661

subpolar North Atlantic, improving the fidelity of the simulations. Indeed these generally compare very well to observations, for example, the formation rate of GSDW in the Control simulation is 0.12 Sv on average – in good agreement with the very broad range of rates (0.1-0.42 Sv) that are available from chloroflurocarbon-based observations[25,26]; and the northward heat transport in the North Atlantic SPG (at 55°N) is 0.66 PW in the Control (1PW=10^{15} W) – in good agreement with observations of 0.6 ± 0.09 PW[32]. Furthermore the length of the new simulations presented here allows a more comprehensive examination of the ocean circulation response and a statistical analysis of the significance of the differences due to polar lows.

A summary of the statistical test results

Supplementary Table 1 summarises the main results from our study. Here we report the monthly mean differences (Δ) between the Perturbation (with polar lows) and Control (without polar lows) integrations for the entire 21-year integration, the last 10 years and the last 5 years, where relevant. The statistical significance of each result is shown by the p-values for both a *two-tailed t-test* and a *two-tailed binomial test*, where p-values <0.05 (95%) are considered statistically significant, and are highlighted in red.

		21 year monthly mean			10 year monthly mean			5 year monthly mean		
		Δ	p-value (t-test)	p-value (binomial)	Δ	p-value (t-test)	p-value (binomial)	Δ	p-value (t-test)	p-value (binomial)
Deep convection										
Greenland Sea	(m)	**-251**	*<0.01*							
Norwegian Sea	(m)	**-121**	*<0.01*							
Iceland Sea	(m)	**-160**	*<0.01*							
Irminger Sea	(m)	**-237**	*<0.01*							
Greenland Sea										
GS gyre	(Sv)	**-0.07**	*0.66*	*<0.01*	**-0.12**	*0.60*	*<0.01*	**-0.27**	*0.51*	*<0.01*
GSDW (vol.)	(km^3)	**-232.48**	*0.94*	-	**1121.84**	*0.50*	*<0.01*	**2867.61**	*0.04*	*<0.01*
Dense water overflows										
DSOW	(Sv)	**-0.03**	*0.24*	*<0.01*	**-0.09**	*0.24*	*<0.01*	**-0.08**	*0.24*	*<0.01*
ISOW	(Sv)	**-0.02**	*0.54*	*<0.01*	**-0.03**	*0.55*	*<0.01*	**-0.05**	*0.48*	*<0.01*
Subpolar North Atlantic										
SPG (whole)	(Sv)	**-0.47**	*<0.01*	*<0.01*	**-0.71**	*<0.01*	*<0.01*	**-0.68**	*<0.01*	*<0.01*
SPG (eastern)	(Sv)	**-0.56**	*<0.01*	*<0.01*	**-0.89**	*<0.01*	*<0.01*	**-0.84**	*0.05*	*<0.01*
Heat Transport	(PW)	**0.01**	*0.02*	*<0.01*	**0.02**	*0.01*	*<0.01*	**0.03**	*<0.02*	*<0.01*

Supplementary Table 1 | A summary of the impact of polar lows on deep convection and ocean circulation. The main changes in our ocean diagnostics and the statistical significances of these results are shown. Note: Δ = monthly mean difference (Perturbation minus Control); GS = Greenland Sea;

GSDW = Greenland Sea Deep Water; vol. = volume; DSOW = Denmark Strait Overflow Water; ISOW = Iceland-Scotland Overflow Water; SPG = SubPolar Gyre. The heat transport is at 55°N.

Supplementary references

27. Uppala, S. M. et al. The ERA-40 re-analysis. *Quart. J. Royal Meteorol. Soc.* **131**, 2961-3012 (2005).

28. Murray, R. J. & Simmonds, I. A numerical scheme for tracking cyclone centres from digital data. Part I: development and operation of the scheme. *Australian Meteorol. Mag.* **39**, 155-166 (1991).

29. Chelton, D. B., Freilich, M. H., Sienkiewicz, J. M. & Von Ahn, J. M. On the use of QuikSCAT scatterometer measurements of surface winds for marine weather prediction. *Mon. Wea. Rev.* **134**, 2055-2071 (2006).

30. Skamarock, W. C. Evaluating mesoscale NWP models using kinetic energy spectra. *Mon. Wea. Rev.* **132**, 3019-3032 (2004).

31. Hoskins, B. J. & Hodges, K. I. New Perspectives on the Northern Hemisphere Winter Storm Tracks. *J. Atmos. Sci.* **59**, 1041-1061 (2002).

32. Ganachaud, A. & Wunsch, C. Large-Scale Ocean Heat and Freshwater Transports during the World Ocean Circulation Experiment. *J. Climate,* **16**, 696-705 (2003).